our results. We tried to keep other acquisition parameters equivalent between 3.0- and 1.5-T imaging, but the bandwidth was higher at 3.0 T. Higher bandwidth results in a reduced signal-to-noise ratio and reduced image distortion. DT imaging at 3.0 T yields a higher signal-to-noise ratio and causes greater magnet susceptibility artifacts owing to the higher static magnetic field strength. We adjusted parameters so that we could use a bandwidth of 1502 Hz per pixel for 3.0-T imaging, which is up to 50% higher than the bandwidth used for 1.5-T imaging. Further optimization of 3.0-T imaging to improve the quality of DT images may be required in the future.

Second, the development of imaging methods to reduce the effects of the crossing-fiber problem, such as high angular DT imaging with high *b* values (38) and diffusion-spectrum imaging (36), is progressing. Other fiber-tracking methods, such as probabilistic tractography to estimate the probability of fiber connections through the data field (39), also are advancing. These advanced methods will affect the results of both 3.0-T and 1.5-T tractography.

In conclusion, DT tractography at 3.0 T enables improved visualization of the corticospinal tract compared with DT tractography at 1.5 T, and 3.0-T tractography of the superior longitudinal fasciculus, corpus callosum, and fornix has some advantages over 1.5-T tractography. Advances in efficient MR sequences are needed to improve the image quality and reliability of 3.0-T DT tractography.

References

1. Basser PJ, Mattiello J, LeBihan D. MR diffusion tensor spectroscopy and imaging. Biophys J 1994;66:259–267.
2. Beaulieu C. The basis of anisotropic water diffusion in the nervous system: a technical review. NMR Biomed 2002;15:435–455.
3. Chenevert TL, Brunberg JA, Pipe JG. Anisotropic diffusion in human white matter: demonstration with MR techniques in vivo. Radiology 1990;177:401–405.
4. Pierpaoli C, Jezzard P, Basser PJ, Barnett A, Di Chiro G. Diffusion tensor MR imaging of the human brain. Radiology 1996;201:637–648.
5. Basser PJ, Pajevic S, Pierpaoli C, Duda J, Aldroubi A. In vivo fiber tractography using DT-MRI data. Magn Reson Med 2000;44:625–632.
6. Mori S, van Zijl PC. Fiber tracking: principles and strategies—a technical review. NMR Biomed 2002;15:468–480.
7. Masutani Y, Aoki S, Abe O, Hayashi N, Otomo K. MR diffusion tensor imaging: recent advance and new techniques for diffusion tensor visualization. Eur J Radiol 2003;46:53–66.
8. Dong Q, Welsh RC, Chenevert TL, et al. Clinical applications of diffusion tensor imaging. J Magn Reson Imaging 2004;19:6–18.
9. Stieltjes B, Kaufmann WE, van Zijl PC, et al. Diffusion tensor imaging and axonal tracking in the human brainstem. Neuroimage 2001;14:723–735.
10. Wakana S, Jiang H, Nagae-Poetscher LM, van Zijl PC, Mori S. Fiber tract–based atlas of human white matter anatomy. Radiology 2004;230:77–87.
11. Clark CA, Barrick TR, Murphy MM, Bell BA. White matter fiber tracking in patients with space-occupying lesions of the brain: a new technique for neurosurgical planning? Neuroimage 2003;20:1601–1608.
12. Yamada K, Kizu O, Mori S, et al. Brain fiber tracking with clinically feasible diffusion-tensor MR imaging: initial experience. Radiology 2003;227:295–301.
13. Huisman TA, Schwamm LH, Schaefer PW, et al. Diffusion tensor imaging as potential biomarker of white matter injury in diffuse axonal injury. AJNR Am J Neuroradiol 2004;25:370–376.
14. Glenn OA, Henry RG, Berman JI, et al. DTI-based three-dimensional tractography detects differences in the pyramidal tracts of infants and children with congenital hemiparesis. J Magn Reson Imaging 2003;18:641–648.
15. Kunimatsu A, Aoki S, Masutani Y, Abe O, Mori H, Ohtomo K. Three-dimensional white matter tractography by diffusion tensor imaging in ischaemic stroke involving the corticospinal tract. Neuroradiology 2003;45:532–535.
16. Tanenbaum LN. 3-T MR imaging: ready for clinical practice [letter]. AJNR Am J Neuroradiol 2004;25:1626–1627.
17. Zhai G, Lin W, Wilber KP, Gerig G, Gilmore JH. Comparisons of regional white matter diffusion in healthy neonates and adults performed with a 3.0-T head-only MR imaging unit. Radiology 2003;229:673–681.
18. Sodickson DK, Manning WJ. Simultaneous acquisition of spatial harmonics (SMASH): fast imaging with radiofrequency coil arrays. Magn Reson Med 1997;38:591–603.
19. Pruessmann KP, Weiger M, Scheidegger MB, Boesiger P. SENSE: sensitivity encoding for fast MRI. Magn Reson Med 1999;42:952–962.
20. Griswold MA, Jakob PM, Heidemann RM, et al. Generalized autocalibrating partially parallel acquisitions (GRAPPA). Magn Reson Med 2002;47:1202–1210.
21. van den Brink JS, Watanabe Y, Kuhl CK, et al. Implications of SENSE MR in routine clinical practice. Eur J Radiol 2003;46:3–27.
22. Jaermann T, Crelier G, Pruessmann KP, et al. SENSE-DTI at 3 T. Magn Reson Med 2004;51:230–236.
23. Naganawa S, Koshikawa T, Kawai H, et al. Optimization of diffusion-tensor MR imaging data acquisition parameters for brain fiber tracking using parallel imaging at 3 T. Eur Radiol 2004;14:234–238.
24. Nagae-Poetscher LM, Jiang H, Wakana S, Golay X, van Zijl PC, Mori S. High-resolution diffusion tensor imaging of the brain stem at 3 T. AJNR Am J Neuroradiol 2004;25:1325–1330.
25. Bastin ME, Armitage PA. On the use of water phantom images to calibrate and correct eddy current induced artefacts in MR diffusion tensor imaging. Magn Reson Imaging 2000;18:681–687.
26. Pajevic S, Pierpaoli C. Color schemes to represent the orientation of anisotropic tissues from diffusion tensor data: application to white matter fiber tract mapping in the human brain. Magn Reson Med 1999;42:526–540.
27. Naidich TP, Valavanis AG, Kubik S. Anatomic relationships along the low-middle convexity. I. Normal specimens and magnetic resonance imaging. Neurosurgery 1995;36:517–532.
28. Mori S, Kaufmann WE, Davatzikos C, et al. Imaging cortical association tracts in the human brain using diffusion-tensor-based axonal tracking. Magn Reson Med 2002;47:215–223.
29. Lazar M, Field AS, Lee J, et al. Lateral asymmetry of superior longitudinal fasciculus: a white matter tractography study (abstr). In: Proceedings of the 12th Meeting of the International Society for Magnetic Resonance in Medicine. Berkeley, Calif: International Society for Magnetic Resonance in Medicine, 2004; 1290.

30. Fera F, Yongbi MN, van Gelderen P, Frank JA, Mattay VS, Duyn JH. EPI-BOLD fMRI of human motor cortex at 1.5 T and 3.0 T: sensitivity dependence on echo time and acquisition bandwidth. J Magn Reson Imaging 2004;19:19–26.

31. Willinek WA, Born M, Simon B, et al. Time-of-flight MR angiography: comparison of 3.0-T imaging and 1.5-T imaging—initial experience. Radiology 2003;229:913–920.

32. Willinek WA GJ, von Falkenhausen M, et al. 3.0T contrast-enhanced, submillimeter MRA of the supraaortic arteries: does the signal gain at high field strength allow to replace the phased array coil by the quadrature body coil? (abstr). In: Proceedings of the 12th Meeting of the International Society for Magnetic Resonance in Medicine. Berkeley, Calif: International Society for Magnetic Resonance in Medicine, 2004; 1523.

33. Graf H, Schick F, Claussen CD, Seemann MD. MR visualization of the inner ear structures: comparison of 1.5 Tesla and 3 Tesla images. Rofo 2004;176:17–20.

34. Hunsche S, Moseley ME, Stoeter P, Hedehus M. Diffusion-tensor MR imaging at 1.5 and 3.0 T: initial observations. Radiology 2001; 221:550–556.

35. Yagishita A, Nakano I, Oda M, Hirano A. Location of the corticospinal tract in the internal capsule at MR imaging. Radiology 1994;191:455–460.

36. Lin CP, Wedeen VJ, Chen JH, Yao C, Tseng WY. Validation of diffusion spectrum magnetic resonance imaging with manganese-enhanced rat optic tracts and ex vivo phantoms. Neuroimage 2003;19:482–495.

37. Wiegell MR, Larsson HB, Wedeen VJ. Fiber crossing in human brain depicted with diffusion tensor MR imaging. Radiology 2000; 217:897–903.

38. Tuch DS, Reese TG, Wiegell MR, Makris N, Belliveau JW, Wedeen VJ. High angular resolution diffusion imaging reveals intravoxel white matter fiber heterogeneity. Magn Reson Med 2002;48:577–582.

39. Behrens TE, Woolrich MW, Jenkinson M, et al. Characterization and propagation of uncertainty in diffusion-weighted MR imaging. Magn Reson Med 2003;50:1077–1088.

Ken-ichiro Kikuta, M.D., Ph.D.
Department of Neurosurgery,
Kyoto University Graduate School
of Medicine,
Kyoto, Japan

Yasushi Takagi, M.D., Ph.D.
Department of Neurosurgery,
Kyoto University Graduate School
of Medicine,
Kyoto, Japan

Kazuhiko Nozaki, M.D., Ph.D.
Department of Neurosurgery,
Kyoto University Graduate School
of Medicine,
Kyoto, Japan

Takashi Hanakawa, M.D., Ph.D.
Human Brain Research Center,
Kyoto University School of Medicine,
Kyoto, Japan

Tsutomu Okada, M.D.
Department of Diagnostic Imaging
and Nuclear Medicine,
Kyoto University
School of Medicine,
Kyoto, Japan

Yukio Miki, M.D., Ph.D.
Department of Diagnostic Imaging
and Nuclear Medicine,
Kyoto University School of Medicine,
Kyoto, Japan

Yasutaka Fushimi, M.D.
Department of Diagnostic Imaging
and Nuclear Medicine,
Kyoto University School of Medicine,
Kyoto, Japan

Hidenao Fukuyama, M.D., Ph.D.
Human Brain Research Center,
Kyoto University School of Medicine,
Kyoto, Japan

Nobuo Hashimoto, M.D., Ph.D.
Department of Neurosurgery,
Kyoto University Graduate School
of Medicine,
Kyoto, Japan

Reprint requests:
Ken-ichiro Kikuta, M.D., Ph.D,
Department of Neurosurgery,
Kyoto University
Graduate School of Medicine,
54 Kawaharacho, Shogoin,
Sakyo-ku, Kyoto
606-8507, Japan.
Email: kikuta@kuhp.kyoto-u.ac.jp

Received, May 18, 2005.
Accepted, September 7, 2005.

EARLY EXPERIENCE WITH 3-T MAGNETIC RESONANCE TRACTOGRAPHY IN THE SURGERY OF CEREBRAL ARTERIOVENOUS MALFORMATIONS IN AND AROUND THE VISUAL PATHWAY

OBJECTIVE: To evaluate of the role of magnetic resonance (MR) tractography on the optic radiation with a 3-T MR unit in the surgery of cerebral arteriovenous malformation (AVM) in and around the visual pathway.

METHODS: Of the 322 patients with cerebral AVMs admitted to our clinic between 1978 and 2005, a study of MR tractography was made on 29 patients. Ten of those patients had AVMs in and around the visual pathway and were included in this study. There were two men and eight women ranging in age from 15 to 64 years (mean age, 34.5 ± 14.8 yr). All of the patients underwent 3-T tractography of optic radiation (OR) and neuro-ophthalmologic evaluation. Four of the 10 patients underwent surgical resection of the AVM. A postoperative 3-T MR study and a neuro-ophthalmologic evaluation was performed 1 month after surgery in most patients.

RESULTS: The preoperative patients for whom tractography demonstrated a continuous bundle of OR from the medial temporal region to the primary visual cortex had minimal or no visual field loss, whereas the patients for whom the tractography did not show a continuous bundle of OR had significant visual loss. The patients for whom tractography in the postoperative study demonstrated a bundle of OR experienced no postoperative deterioration of the visual field loss, whereas the patients for whom tractography did not demonstrate a bundle of OR exhibited significant visual field loss.

CONCLUSION: This technique is thought to be useful in confirming the integrity of and localizing deviated tract and in evaluating the surgical risk, especially for nonhemorrhagic AVMs in and around the visual pathways, taking some limitations of this method into consideration.

KEY WORDS: Arteriovenous malformation, Diffusion tensor tractography, Optic radiation, Surgical indication, 3-Tesla magnetic resonance imaging

Neurosurgery 58:331-337, 2006 DOI: 10.1227/01.NEU.0000195017.82776.90 www.neurosurgery-online.com

In palliative treatment of arteriovenous malformations (AVMs), there is an inverse increase in the risk of bleeding (12). Thus, in the surgery of AVMs, complete resection of the nidus is always required even if other intraaxial lesions do not allow complete resection to avoid postoperative deficits. Surgical indication for AVMs usually is determined according to the risk of postoperative deficits when complete resection is accomplished. Surgical indication for AVMs is usually determined according to the risk of postoperative deficits when complete resection is accomplished.

Recent advances in magnetic resonance (MR) technology have made it possible to describe major neural tracts in the white matter by diffusion tensor tractography (2, 4, 13, 14, 21), including the visual pathways in the occipitotemporal connections (10). Diffusion corresponds to the random motion of water molecules. Although the tissue exhibits the property of anisotropy in the region where

diffusion of water varies significantly with direction, it shows low anisotropy (expressed as isotropic) in the regions where diffusion is similar in all directions (11, 20). Anisotropy can be quantified by one of several indices, including fractional anisotropy (FA). These indices are derived from a full description in the region of interest (the diffusion tensor) obtained by measuring changes in the nuclear MR signal with diffusion sensitization along at least six noncollinear directions. In an axonal cylinder, water diffusion is faster along the axon than across it, probably because of the presence of structures, including the axonal membrane and the neurofilamentary cytoskeleton, which behave as barriers to diffusion. Because fiber tracts are composed of collections of similarly oriented axons that generally exhibit high anisotropy values, FA reflects the integrity of fiber tracts. Diffusion within each voxel can be described by three mutually perpendicular eigenvectors, whose magnitude is given by three corresponding eigenvalues. The eigenvalues are the three principal diffusion coefficients measured along the three eigenvector directions that define the local fiber frame of references for that voxel. The direction of fiber is thus given by the eigenvector of the largest eigenvalue of the diffusion tensor (11, 20).

We reported that a 3-T MR unit can describe most of neural tracts more clearly than a 1.5-T unit (8, 15). Tractography of the four neural tracts (corticospinal tract, superior longitudinal fasciculus, corpus callosum, and fornix) described by a 3-T unit was compared with that by a 1.5-T unit in the degree of inspective recognition by the observers, in the quantitative number of fiber bundles, and in the right-left asymmetry of the number of bundles. The 3-T unit showed significant better performance in all three aspects in describing the corticospinal tract, and in at least one of the three aspects in describing other three neural tracts (15). This study provides the results of early experiences using 3-T MR tractography in the surgery of cerebral AVMs in and around the visual pathway.

PATIENTS AND METHODS

Patients

Of the 322 patients with AVMs admitted to our clinic between 1978 and 2005, 29 underwent 3-T MR tractography. Ten of those patients had AVMs in and around the visual pathway and were included in this study. There were two men and eight women ranging in age from 15 to 64 years (mean age, 34.5 ± 14.8 yr). Three patients experienced hemorrhagic onset. Four had migraine-like episodes and four exhibited some visual field loss. The location of the AVMs was the occipital pole in three patients, the medial portion of the occipital lobe in one, the lateral portion of the occipital lobe in two, the posterior portion of the temporal lobe in three, and the thalamus in one. The Spetzler-Martin grade of the AVMs was I in two patients, II in three patients, III in three patients, and IV in two patients. The characteristics of the patients are shown in *Figure 1*. Four of the 10 patients (Patients 1–4) underwent surgical treatment. Surgical resection alone was performed in Patients 1, 2, and 4, and surgery after embolization was performed in Patients 3. The characteristics of the patients who had surgical treatment are shown in *Figure 2*. Complete obliteration of the lesion was confirmed in all surgical cases by postoperative angiography.

Neuro-ophthalmologic Evaluation

A Goldmann perimetry was performed in all 10 patients to assess visual field loss. Postoperative examinations were performed once 1 month after surgery in two patients, twice in one patient 1 week and 1 month after surgery, and twice in one patient 1 month and 5 months after surgery. Visual field defects of the patients were classified into five grades (normal, incomplete quadrantanopia, complete quadrantanopia, incomplete hemianopia, complete hemianopia) according to the amount of loss reported previously (6, 7) (*Figs. 1* and *2*).

Imaging Methods

All patients were studied before surgery with the same 3-T MR scanner (Magnetom Trio; Siemens, Erlangen, Germany). In four surgical patients, a postoperative MR study was carried out once 1 month after surgery in three patients and twice in one patient 1 month and 5 months after surgery. Images were obtained with axial T2-weighted turbo spin echo sequences (TR/TE = 8400/108 ms; flip angle, 150°; matrix, 512 × 448; field of view, 22 cm; 40 slices; slice thickness, 2.3 mm; interslice gap, 0.7 mm and twice averaging) and with axial T1-weighted three-dimensional magnetization-prepared rapid acquisition gradient-echo (MPRAGE) sequences (TR/TE/TI = 2000/4.4/990 ms; flip angle, 8°; matrix, 256 × 240; field of view, 24 cm; 208 slices; slice thickness, 1 mm, no interslice gap and single averaging). At the same time, thin-section diffusion-tensor imaging was performed. The diffusion-tensor imaging acquisition time was 4 minutes and 24 seconds. A single-shot spin echo echo-planar imaging technique was used (repetition time/echo time = 5300/79 ms) with a motion-probing gradient in 12 orientations, a *b* value of 700 seconds/mm^2, and four times averaging. The generalized autocalibrating partially parallel acquisitions algorithm was applied for parallel imaging, with a reduction factor of 2 and 24 additional autocalibrating phase-encoding steps in the center of *k* space. The reconstructed images had a 128 × 128 matrix. A total of 40 sections were obtained with a thickness of 3 mm without interslice gaps. The imaging field center for T2-weighted images, MPRAGE, and diffusion tensor imaging were adjusted to the same location.

Data Processing

We transferred the diffusion-tensor imaging data to an offline workstation for data analysis. DTI studio software version 2.03 (H. Jiang, S. Mori; Department of Radiology, Johns Hopkins University) was used for tensor calculations (11, 20). After calculating the six independent elements of the 3 × 3 tensor and diagonalization, three eigenvalues and eigenvectors were

case	1	2	3	4	5	6	7	8	9	10
age	38	27	29	28	15	37	55	64	25	27
gender	F	F	F	F	F	F	F	M	M	F
onset	headache, scintilating scottoma	hemorrhage	headache, scintilating scottoma	hemorrhage	headache, scintilating scottoma	hemorrhage	headache, scintilating scottoma	incidental	headache	vertigo
size (cm)	2	2	4	4	4	4	4	2	4	5
side	L	R	R	R	R	R	R	R	R	L
location	occipital, medial	temporal, posterior	occpital, lateral	temporal, posterior	occipital, lateral	thalamus	occipital pole	occipital pole	temporal, posterior	occipital pole and thalamus
S-M grade	I	I	II	III	III	IV	IV	II	II	III
visual field loss	incomplete homonimous quadrantanopia	complete homonimous hemianopia	none	none	none	complete honomimous quadrantanopia	none	none	none	complete homonimous hemianopia
3-tesla MR tractgraphy of OR	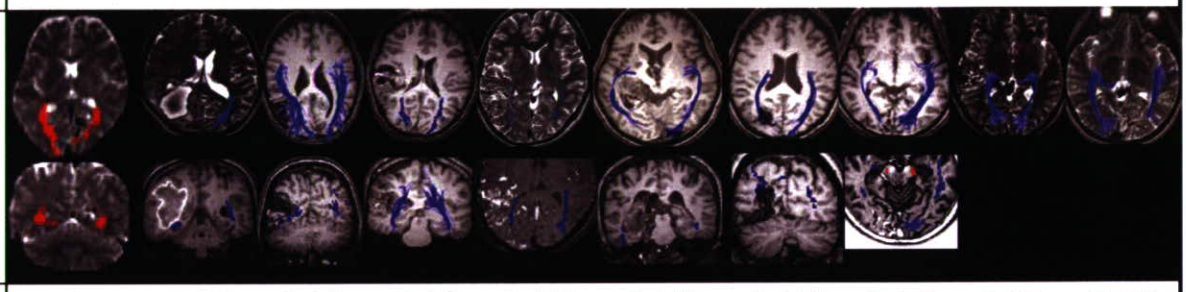									
State of OR	Grade II	Grade V	Grade II	Grade I	Grade III	Grade IV	Grade III	Grade II	Grade I	Grade V
	running just besides the nidus	disrupted	running just besides the nidus	running completely apart from the nidus	passing through the nidus	fairly described on the tractgraphy	passing through the nidus	running just besides the nidus	running completely apart from the nidus	disrupted

FIGURE 1. *Diagram summarizing the 10 patients with AVMs in and around the optic radiation who underwent a 3-T MR study. It gives the age, sex, type of onset, side, location, Spetzler-Martin grade of the lesion, surgical indication, amount of preoperative visual field defect, MR tractography of OR, and interpretation of the findings of tractography.*

obtained. The eigenvector associated with the largest eigenvalue was assumed to represent the intravoxel fiber orientation. An FA map and a directional color-coded map were synthesized. Starting from a particular region of interest, one can follow the direction of the principal eigenvector, thus following the corresponding fiber. Translation of eigenvectors into neuronal trajectories was achieved by a technique known as the fiber assignment by continuous tracking method, which was initially described by Mori et al. (11). The procedure for mapping neural connections is performed by designating two regions of interest in the three-dimensional space on DTI studio software. Region of interest segmentation was performed by one author (TO). The region of interest placement starts at the lateral geniculate ganglion in bilateral mesial temporal region on coronal b = 0 images. Then a secondary region of interest was added at the bilateral occipital lobe on the coronal images. The optic radiation (OR) was identified as a green color area abutting the trigone of lateral ventricle in the temporo-occipital deep white matter on a coronal color-coded map (17, 20). The secondary regions of interest were placed at the area as described on a coronal color-coded map. This method was useful when the AVMs were situated close to the primary visual cortex and the primary visual cortex was difficult to identify based on the sulcal patterns. Tracking was terminated when it reached a pixel with low FA (<0.2) or a predetermined trajectory curvature between two contiguous vectors (inner product, <0.75). Fiber tracts that passed through both regions of interest were designed to be the final tract of interest. The traced fiber tracts in this study included OR and temporal part of inferior occipito-frontal fasciculi. There are the arcuate fibers and the fibers with downward projection from the splenium of corpus callosum (tapetum) that courses near the OR/inferior occipitofrontal fasciculus (IOFF) complex in the temporal lobe. These fibers are the structures localized lateral to the OR/IOFF complex and along with the z axis of MRI scanner, whereas the OR/IOFF complex exists mainly along with the *y* axis. Therefore, their presentation and orientation apparently can be discriminated from those of the OR/IOFF complex on the FA map and can be deleted selectively on the software (7, 15). A typical tract reconstruction by using a two-region of interest method required approximately 1 minute by using a 3.2-GHz Pentium IV workstation (Dell, Austin, TX). The entire data postprocessing time for ORs on both hemispheres took approximately 10

case	age	gender	intervention	Preopeartive study		Postoperative status		
				state of the OR	visual field loss	state of the OR (timing of the study)		visual field loss (timing of the study)
1	38	F	surgery	running just lateral to the nidus	incomplete quadrantanopia	preserved (1 mo. after surgery)	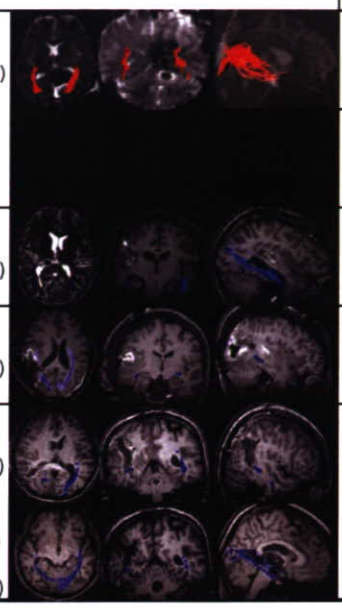	complete quadrantanopia (1 wk. after surgery) incomplete quadrantanopia (1 mo. after surgery)
2	28	F	surgery	running apart from the nidus	no defect	preserved (1mo. after surgery)		no defect (1mo. after surgery)
3	29	F	surgery after embolization	running just inferomedial to the nidus	no defect	disrupted (1mo. after surgery)		incomplete hemianopia (1mo. after surgery)
4	27	F	surgery	disrupted	conplete hemianopia	remained disrupted (1mo. after surgery) appeared to be running just benieth the nidus (5 mo. after surgery)		conplete hemianopia (1mo. after surgery) incomplete quadrantanpoia (5 mo. after surgery)

FIGURE 2. *Diagram summarizing four patients who received surgical treatment for AVMs. It provides the age, sex, type of onset, amount of preoperative and postoperative visual field defect, postoperative MR tractography of OR, and interpretation of preoperative and postoperative tractography.*

to 15 minutes after completion of the examination, including the data transfer to the off-line workstation.

Evaluation of the State of OR on Tractography and the Geometrical Relationship between the Nidus and the OR

When the OR could be described as a continuous bundle, the geometrical relationship between the nidus and the OR was evaluated by fusing the images of tractography and those of MPRAGE or T2-weighted images. The field center for T2-weighted image, MPRAGE, and diffusion tensor imaging were adjusted, and a fusion image was obtained using DTI studio by simple overlay. Our diffusion tensor imaging obtained with a Siemens MR scanner had low eddy current geometric distortion (1), and the parallel imaging technique also contributed to the lower magnetic susceptibility related artifact. A simple overlay is enough for creating fusion images with the same field center. OR tractography was classified into five grades as described: Grade I, the OR was running completely apart from the nidus; Grade II, the OR was running just beside the nidus; Grade III, the OR was passing through the nidus or projecting into the nidus. When the OR could not be described clearly, the state of OR description was graded as follows: Grade IV, the OR was fairly described on the tractography; Grade V, the OR cannot be described completely (disrupted).

RESULTS

Relationship between the Findings of Tractography and the Amount of Visual Field Loss before Surgery

The OR could be described as a continuous bundle on preoperative tractography in seven patients. The OR coursed apart from the nidus in two patients and just beside the nidus in three patients and passed through the nidus in two patients. In the remaining three patients, the OR was fairly described on the tractography in one patient and was disrupted by the hematoma or the huge nidus in two patients. The first seven patients had no or minimal visual field loss at presentation, whereas the remaining three patients exhibited severe visual field loss at presentation. As for the four patients with migraine-like episodes at presentation, the OR coursed just beside the nidus or passed through the nidus.

Relationship between the Findings of Tractography and the Amount of Visual Field Loss after Surgery

Among the four patients who underwent surgical treatment, the OR was preserved in the postoperative study 1 month after surgery in two patients (Patients 1, 2) (*Fig. 2*). The two patients exhibited no deterioration of visual field loss 1 month after surgery. In Patient 1, transient worsening of visual field loss occurred within 1 week of surgery, but the deficits

were improved to preoperative status by 1 month after surgery. In Patient 3, a large part of the occipital lobe had to be removed because of intraoperative normal perfusion pressure breakthrough. The OR could not be described on the postoperative study 1 month after surgery, and deterioration of visual field loss occurred after surgery. In Patient 4, the OR was disrupted by a hematoma both in the preoperative study and in the study 1 month after surgery. However, the OR seemed to be described in the study at 5 months after surgery in accordance with the shrinkage of the hematoma. The amount of visual field loss of the patient was unchanged 1 month after surgery, but was much reduced 5 months after surgery (*Fig. 2*).

Preoperative and Postoperative FA Maps and Quantitative FA Values in the Representative Patients

In Patient 1, ORs on both sides in the preoperative (*Fig. 3A*) and the postoperative OR tractography (*Fig. 3B*) were well visualized on the three-dimensional view of OR tractography, the two-dimensional view of OR tractography overlaid on axial FA map, and on axial MPRAGE images. Postoperative FA values along the tract did not differ from preoperative ones. In Patient 3, preoperative and postoperative left OR tractography were well visualized, but postoperative right OR tractography seemed to be damaged (*Fig. 4*). Patient 3 exhibited lower FA values in postoperative tractography than preoperative tractography in the affected hemisphere.

DISCUSSION

In the surgery of cerebral AVMs, complete obliteration is always required because palliative treatment inversely increases the risk of bleeding (12). We previously reported that a dissection technique with minimal coagulation that preserves the intranidal venous drainage is important for avoiding postoperative neurological deterioration (3). In addition, one of the most important factors of a favorable surgical outcome is that surgical indication is determined according to the risk of postoperative neurological aggravation when complete resection is accomplished.

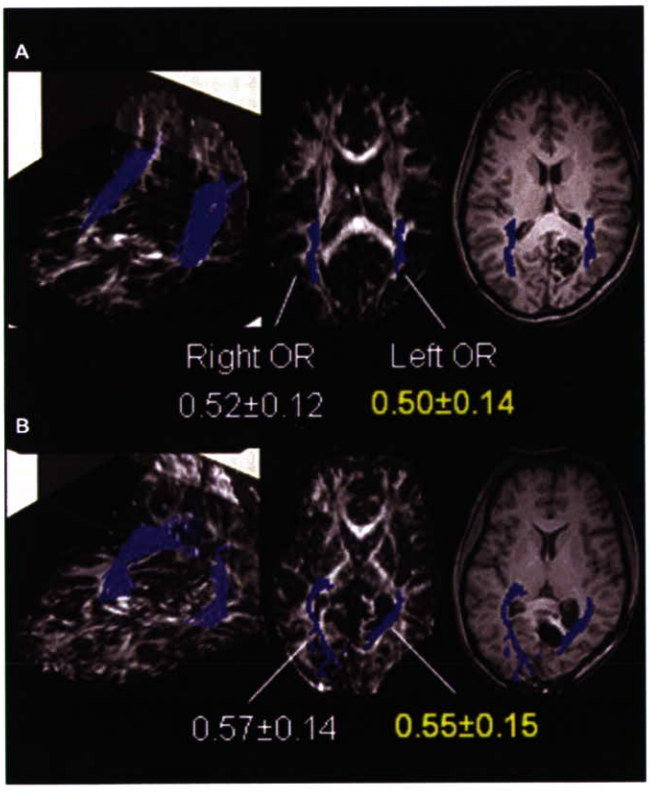

FIGURE 3. A, *preoperative and* (B) *postoperative images of Patient 1, who had a left occipital AVM:* (left) *Three-dimensional view of OR tractography,* (middle) *two-dimensional view of OR tractography overlaid on axial FA map, and* (right) *axial MPRAGE images. Both preoperative and postoperative OR tractography are well visualized on both sides, and postoperative FA values (mean ± standard deviation) along the tract on the affected side do not differ from preoperative values.*

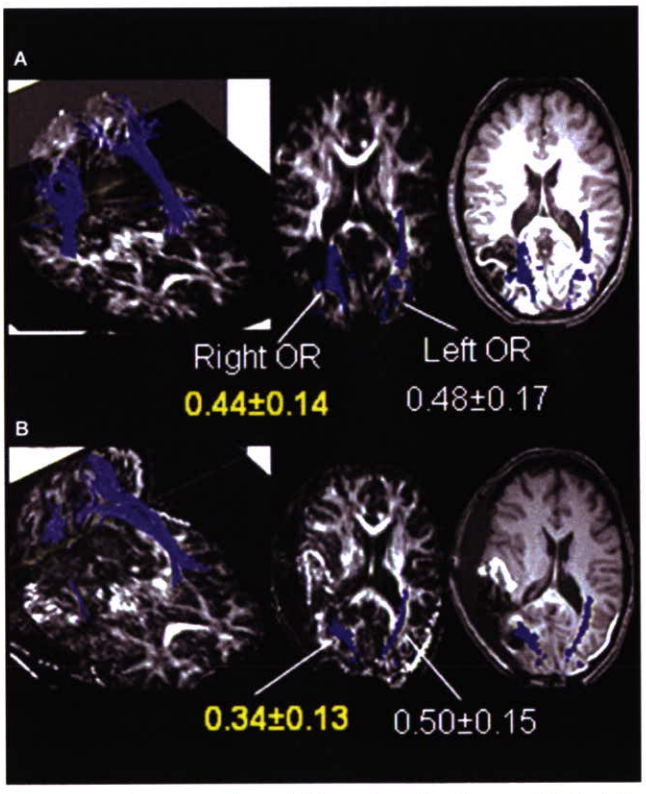

FIGURE 4. A, *preoperative and* (B) *postoperative images of Patient 3, who had a right occipital AVM:* (left) *Three-dimensional view of OR tractography,* (middle) *two-dimensional view of OR tractography overlaid on axial FA map, and* (right) *axial MPRAGE images. Preoperative and postoperative left OR tractography are well visualized, but the postoperative right OR exhibits lower FA values in postoperative tractography than preoperative tractography in the affected hemisphere.*

MR tractography by diffusion tensor imaging has realized visualization of the major neural tracts in the white matter both in physiological and pathological conditions (2, 4, 10, 13, 14, 19). Prognosis of motor function in the patients with lenticulostriate infarcts was related to the geometrical relationship between the lesion and motor fibers on the tractography (13). MR tractography visualized sensorimotor fibers in the patients with AVMs situated near sensorimotor cortices (19). Use of a neuronavigation system combined with the tractography of the corticospinal tract in tumor surgery also was reported (4, 14).

In this study, we used a 3-T MR unit in the evaluation of the surgical risk of AVMs situated near the OR, because a 3-T unit can describe most of neural tracts more clearly than 1.5-T units (8, 15). The patients exhibited minimal or no visual field loss when the OR could be described as a continuous bundle. The patient for which the OR was disrupted or fairly described on the tractography exhibited severe visual field loss. The findings of postoperative tractography also corresponded with the amount of visual field loss. These findings suggest that estimation of the state of OR and evaluation of the geometrical relationship between the nidus and the OR are useful for determining the surgical risk of AVMs in and around the visual pathways. Currently, we exclude patients who exhibit minimal or no preoperative visual field loss from the surgical indication of AVMs in and around the visual pathways when the OR is described as a bundle passing through or projecting to the nidus.

Postoperative transient worsening of visual field loss was observed in two patients. In one patient, transient worsening occurred 1 week after surgery. The OR could be described at 1 month after surgery and visual field loss of the patient recovered to the preoperative status. In this patient, transient worsening might have been caused by mechanical injury by surgical manipulation or by transient change of regional blood flow around the OR. In three of the four patients who underwent surgery, the amount of visual field loss correlated to the state of OR in the study 1 month after surgery. Tractography of the OR also may be useful to predict the prognosis of postoperative visual field deficits and the optimal time for the study to estimate the state of OR at 1 month after surgery.

Functional translocation sometimes occurs in the brain of patients with cerebral AVMs (5, 9, 19). In this series, there were two patients (Patients 2 and 8) exhibiting no visual field loss such that the course of the OR was deviated by the nidus. The OR passed through the nidus in two patients (Patients 5 and 7) who also exhibited visual field loss. Although further investigation is necessary, tractography of the OR may indicate whether the functions for vision remain in the neural tissue within the nidus. That is critical in determining surgical indication of AVMs.

There are three limitations in this study. Visual loss of the patients with disruption of the OR by hematoma on the tractography at presentation seemed to improve in accordance with the shrinking of the hematoma. However, description of the OR was less in all patients with hematoma (Patients 2, 4, and 6) than in patients without hematoma. These observations show not only that the description of the OR in the tractography corresponded to the visual functions, but also suggest the possibility that the tractography in our method has less ability to describe the tract under existence of hematoma. Our study potentially has the technical concerns of a single-shot technique regarding possible susceptibility artifacts from the hematoma that may cause signal intensity drop-off around the nidus on the source diffusion tensor images. Our method should be feasible for most nonhemorrhagic AVMs, and evaluation of the tractography should be performed at least after the hematoma has been completely absorbed in those with hematoma.

Some investigators may recommend higher performance of the tractography in a higher number of directions instead of 12 directions in describing the tracts with severely curved or tortuous projection, such as motor fibers of hands in the corticospinal tract and Meyer's loop in the visual pathway. Because we performed the tractography in 12 directions in this study, it was possible that a part of the OR with a severely curved course (Meyer's loop) could not be estimated well. Although we have preliminary data indicating that description of the OR by tractography in 40 and in 81 directions did not significantly differ from by the tractography in 12 directions, this is another limitation of this study that should be examined in the future.

The third limitation is that the grading of the state of OR was determined according to visualization of the tract. It is very difficult to be certain if the tract is really destroyed or disrupted, especially when the OR cannot be visualized on the tractography (Grade V). There is a report of tumor cases suggesting that disruption of the corticospinal tract (CST) on the tractography does not always mean the functional disruption of the tract and that location of CST probed by motor evoked potential often was apart from the corresponding site where tractography is indicated (14). However, we recently reported that location of the CST indicated by intraoperative motor evoked potential corresponded to the site where the tractography is indicated in most patients of our series, mainly patients with nonneoplastic lesions (16). There is a possibility that tractography in patients with tumor cannot reflect the function of the tract so correctly as in patients with AVMs because histopathological change, such as perifocal edema or infiltration of the tumor, often exists in the white matter of tumor patients. Quantitative FA values have a potential to enable the functional evaluation of the tract (18), and an FA value of approximately 0.20 has been reported to be the optimal trackability threshold of the CST (6), which was the same value of the threshold used in our study. This issue will be resolved in the future by the accumulation of data regarding correlation between the function of the tract and the quantitative FA values.

CONCLUSION

In summary, this technique is thought to be useful in confirming the integrity and to localize deviated tract and in

evaluating surgical risk, especially in patients with nonhemorrhagic AVMs in and around the visual pathways, taking some limitations of this method into consideration.

REFERENCES

1. Bastin ME, Armitage PA: On the use of water phantom images to calibrate and correct eddy current induced artefacts in MR diffusion tensor imaging. **Magn Reson Imaging** 18:681–687, 2000.
2. Cabanis EA, Iba-Zizen MT, Nguyen TH, Bellinger L, Stievenart JL, Yoshida M: The visual pathways, from anatomical MRI to physiological with (f)MRI and tractography with diffusion tensor MRI (DTMRI). **Bull Acad Natl Med** 188:1153–1169, 2004.
3. Hashimoto N: Microsurgery for cerebral arteriovenous malformations: A dissection technique and its theoretical implications. **Neurosurgery** 48:1278–1260, 2001.
4. Kinoshita M, Yamada K, Hashimoto N, Kato A, Izumoto S, Baba T: Fiber-tracking does not accurately estimate size of fiber bundle in pathological condition: Initial neurosurgical experience using neuronavigation and subcortical white matter stimulation. **Neuroimage** 25:424–429, 2005.
5. Kombos T, Pietila T, Kern BC, Kopetsch O, Brock M: Demonstration of cerebral plasticity by intra-operative neurophysiological monitoring: Report of an uncommon case. **Acta Neurochir (Wien)** 141:885–889, 1999.
6. Kunimatsu A, Aoki S, Masutani Y, Abe O, Hayashi N, Mori H: The optimal trackability threshold of fractional anisotropy for diffusion tensor tractography of the corticospinal tract. **Magn Reson Med Sci** 3:11–7, 2004.
7. Kupersmith MJ, Vargas ME, Yashar A, Madrid MRN, Nelson K, Seton A: Occipital arteriovenous malformations: Visual disturbances and presentation. **Neurology** 46:953–957, 1996.
8. Larsson EM, Stahlberg F: 3 Tesla magnetic resonance imaging of the brain. Better morphological and functional images with higher magnetic field strength [in Swedish]. **Lakartidningen** 102:460–463, 2005.
9. Lazar RM, Marshall RS, Pile-Spellman J, Hacein-Bey L, Young WL, Mohr JP: Anterior translocation of language in patients with left cerebral arteriovenous malformation. **Neurology** 49:802–808, 1997.
10. Marco C, Derek KJ, Rosario D, Dominic H: Occipito-temporal connections in the human brain. **Brain** 126:2093–2107, 2003.
11. Mori S, van Zijl PC: Fiber tracking: principles and strategies—a technical review. **NMR Biomed** 15:468–480, 2002.
12. Miyamoto S, Hashimoto N, Nagata I, Nozaki K, Morimoto M, Taki W: Posttreatment sequelae of palliatively treated cerebral arteriovenous malformations. **Neurosurgery** 46:589–594, 2000.
13. Nakagawa M, Nishimura T: MR tractography for the evaluation of functional recovery from lenticulostriate infarcts. **Neurology** 64:108–113, 2005.
14. Nimsky C, Ganslandt O, Hastreiter P, Wang R, Benner T, Sorensen AG: Preoperative and intraoperative diffusion tensor imaging-based fiber tracking in glioma surgery. **Neurosurgery** 56:130–137, 2005.
15. Okada T, Miki Y, Fushimi Y, Hanakawa T, Kanagaki M, Yamamoto A: Diffusion tensor fiber tractography: Intra-individual comparison of 3 T and 1.5 T. **Radiology** (in press).
16. Okada T, Mikuni N, Miki Y, Kikuta K, Urayama S, Hanakawa T: Integration of diffusion tensor tractography of the corticospinal tract using 3T with intraoperative white matter stimulation mapping: Preliminary results to validate corticospinal tract localization. **Radiology** (in press).
17. Pajevic S, Pierpaoli C: Color schemes to represent the orientation of anisotropic tissues from diffusion tensor data: Application to white matter fiber tract mapping in the human brain. **Magn Reson Med** 42:526–540, 1999.
18. Shimorry JS, Mckinstry RC, Akbudak E, Aronovitz JA, Snyder AZ, Lori NF: Quantitative diffusion-tensor anisotropy brain MR imaging: Normative human data and anatomic analysis. **Radiology** 212:770–784, 1999.
19. Turski PA, Cordes D, Mock B, Wendt G, Sorenson JA, Fitzurka-Quigley M: Basic concepts of functional MR imaging of arteriovenous malformations. **Neuroimaging Clin N Am** 8:371–381, 1998.
20. Wakana S, Jiang H, Nagae-Poetsce LM, Peter CM, van Zijl PC, Mori S: Fiber tract-based atlas of human white matter anatomy. **Radiology** 230:77–87, 2004.
21. Yamada K, Kizu O, Ito H, Kubota T, Akada W, Goto M: Tractography for arteriovenous malformations near the sensorimotor cortices. **AJNR Am J Neuroradiol** 26:598–602, 2005.

COMMENTS

This study investigates 10 patients with cerebral arteriovenous malformations (AVMs) that were intimate with the optic radiations. Three presented with hemorrhage, and four patients underwent surgical excision. Using 3-T magnetic resonance tractography, the status of the optic radiations was determined both at presentation and after surgical resection in the four patients. There was excellent correlation between the integrity of the optic radiations as imaged on the magnetic resonance studies and the status of the visual fields. Although these results are not surprising, 3-T magnetic resonance tractography may be a useful technique to predict which patients are likely to experience visual field loss after surgical resection of AVMs that are adjacent to the optic radiation or visual cortex.

Robert A. Solomon
New York, New York

Diffusion tensor imaging is a potentially valuable tool for preoperative planning, and may provide information that could be clinically important and that is virtually impossible to obtain with conventional anatomical techniques, such as T1, T2 and flair imaging. This method uses information obtained from anisotropic diffusibility of the water in the white matter tracts. Nowadays, the diffusion tensor technique is used increasingly, as it is present in most commercially available magnetic resonance scanners. This study by Kikuta et al. provides some interesting information, such as the good correlation between the integrity of the odds ratio in the tractography and the absence of important visual field defect, at least anecdotally. Other than the good correlation between what they called disrupted tract and the visual field defect, there are some technical limitations that deserve comment, for instance the magnetic field distortion in the hemorrhagic cases that could be responsible for misinterpretation of the real odds ratio status. Also, we do not know for sure if the tract is completely or only partially represented in the color-coded map. That is why the role of the diffusion tensor imaging in planning and postoperative follow-up still has to be defined. The fast technical improvement in software and hardware will certainly shorten this time and, in the near future, we will really be able to inform about the real status of the white matter tracts.

Nelson F. Ferreira
Evandro P. de Oliveira
São Paulo, Brazil

The authors have used a novel imaging technique which has proven useful in both the preoperative prediction of visual loss associated with resection of AVMs in and near the optic radiations and in the postoperative differentiation between permanent deficits and those likely to improve with time. Although their series is small, the findings are compelling. If they are confirmed by other surgeons, magnetic resonance tractography may be a very helpful addition to our evaluation armamentarium in selected patients.

Duke S. Samson
Dallas, Texas

9 革新的診断・治療へのアプローチ

―膜透過性・標的特異性を有する融合タンパク質を用いたイメージング・ターゲティング―

■近藤　科江・原田　浩・平岡　真寛
京都大学医学研究科・腫瘍放射線科学

近藤　科江
1989年大阪大学で医学博士修得。90年学振特別研究員（がん）、93年ERATO岡山細菌変換プロジェクト研究員。99年京都大学医学研究科助手。2004年京都大学医学研究科COEプロジェクト"病態解明を目指す基礎医学研究拠点"特任助教授。
研究テーマは、低酸素がん細胞・アポトーシスの解析と病態イメージング。趣味は登行。

Key words：低酸素がん細胞、膜透過ドメイン（PTD；Protein transduction domain），HIF-1，酸素濃度依存的分解（ODD; Oxygen-dependent degradation）

Abstract

低酸素が問題になる疾患には、脳・心筋梗塞や閉塞性末梢動脈硬化症といった虚血性疾患のみならず、難治性固形腫瘍が含まれる。固形腫瘍には、細胞増殖と血管新生の不均衡に起因する「低酸素領域」が存在する。低酸素領域にあるがん細胞は、放射線や抗がん剤に感受性が低く、治療効果不良の主因であるばかりでなく、浸潤・転移・再発の温床となっている。しかし、低酸素環境は正常組織には存在しないため治療標的となりうる。我々は、低酸素環境下にある細胞内で特異的に安定化する融合タンパク質を開発し、それを用いることにより、低酸素細胞のイメージング・ターゲティング研究を行っている。本稿では、固形腫瘍を対象にした研究について紹介する。

はじめに

医学の進歩に伴い、がんの診断・治療技術も年々進歩してきている一方で、我が国では、世界のどの国も経験したことのない速度で人口の高齢化が進行している。これが我が国でがんが増える第一の要因になっている。血液検査、内視鏡、画像診断等の技術の向上により、多くのがんが早期に発見できるようになってきたが、「手軽に、どのがんでも」というところまでは至っていない。我々の研究は、早期診断・早期治療に革新的イメージング・ターゲティング技術を提供することにより、がん撲滅に寄与することを目的としている。

1. 腫瘍内低酸素領域

固形がんには、非常に小さながん（数ミリ以下）でも通常ではありえないような低酸素状態のがん細胞が存在する。それは、がん細胞の増殖に血管新生が追いつかないために、血流からの酸素や栄養が十分行き渡らない領域が生じるためで、酸素も栄養も枯渇して死んでしまったがん細胞と増殖しているがん細胞の境界の極めて限られた領域に存在する（図1）。この低酸素がん細胞は、過酷な環境に順応するために、増殖は停止し、代謝も解糖系を用いて省エネルギー化し、いわば冬眠状態にある。それだけであれば、これら低酸素がん細胞は注目に値しないのであるが、これらの細胞はがん治療の抵抗性の指標となるほど、抗がん剤や放射線治療に抵抗性を示す。従って、癌治療が終わった後も生き残り、再発の温床となる可能性が指摘されている。更

Imaging and targeting with a novel fusion protein possessing membrane permeability and target-specificity: Shinae Kondo, Hiroshi Harada, Masahiro Hiraoka, Department of Therapeutic Radiology and Oncology, Kyoto University Graduate School of Medicine

に、生き延びるために様々な因子（例えばＶＥＧＦ，ＴＧＦ－β，　ＦＧＦ，　ＩＧＦ）を分泌して、血管新生を促したり、転移や浸潤に関わったりして、腫瘍全体の悪性度を高める働きをする。故に、低酸素がん細胞は癌治療を行う上で、見逃すことができない標的であると同時に、低酸素がん細胞が存在する微小環境は『正常組織ではありえない』という点で絶好の標的（環境標的）となりうる。

2. 酸素濃度依存的制御機構

この低酸素がん細胞には、極めて興味深いタンパク質が存在する。そのタンパク質はＨＩＦ－１αと呼ばれ、転写因子ＨＩＦ－１を構成する２つのサブユニットのひとつで、低酸素環境で安定化し、通常の酸素環境下（有酸素環境）で速やかに分解される。そのためＨＩＦ－１は低酸素環境下で機能し、低酸素特異的に応答する一連の遺伝子の発現を誘導する。それらの遺伝子は、低酸素がん細胞が過酷な微小環境に順応するために必要な因子や上記のがん悪性化に関与する因子をコードしている。

我々は、ＨＩＦ－１αタンパク質の酸素濃度依存的分解（ＯＤＤ）制御機構に着目した。2001年に新たなプロリン水酸化酵素が発見さ

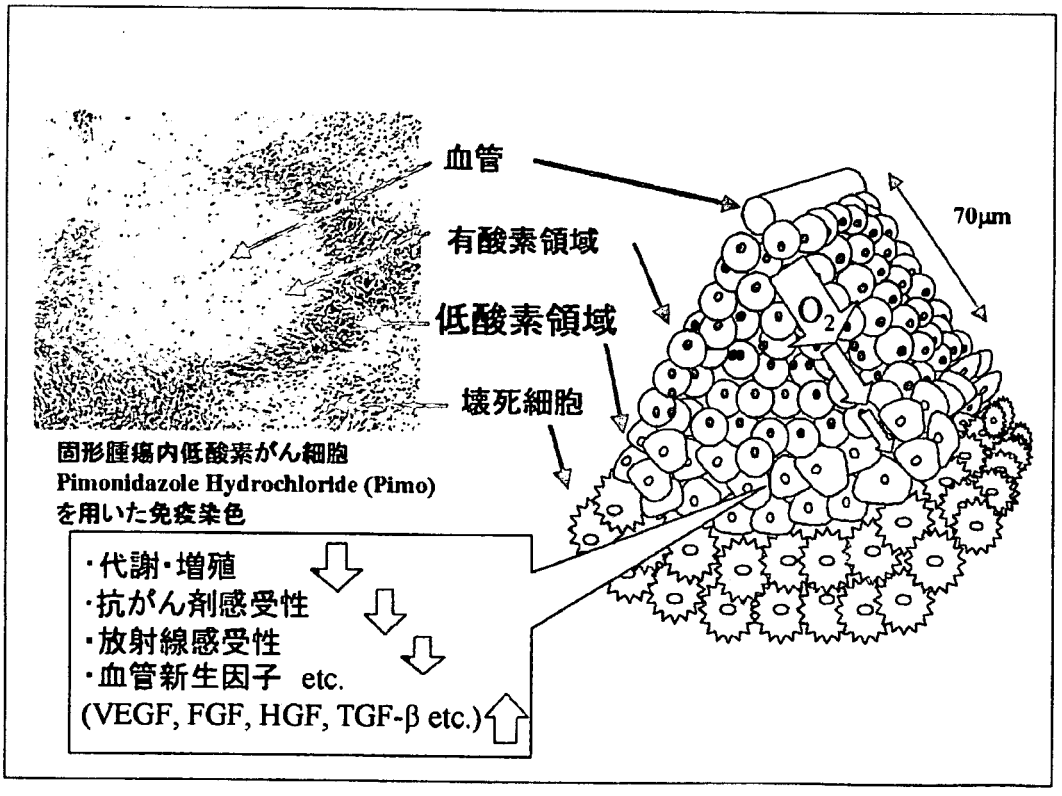

図1　固形腫瘍内低酸素領域

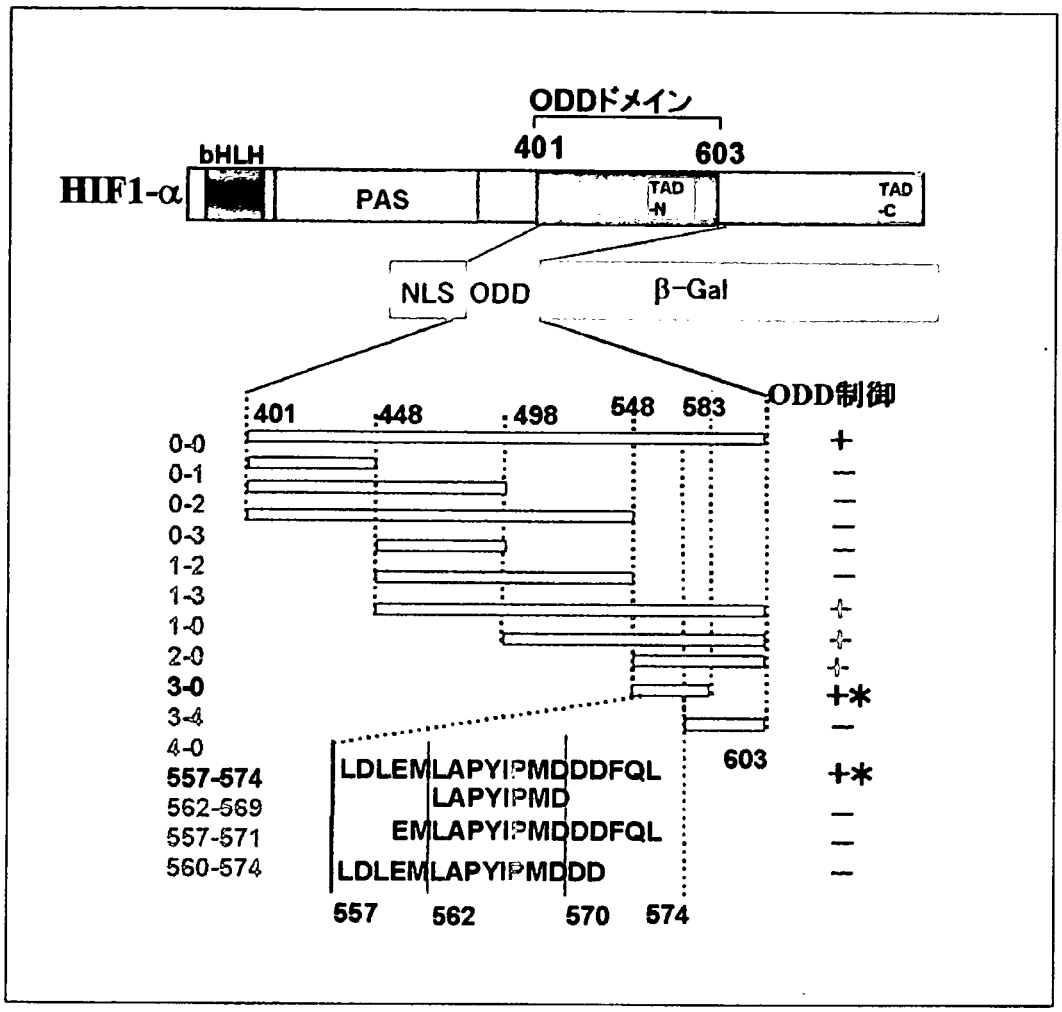

図2　ODD融合タンパク質のODD制御

れ、この制御機構は分子レベルで詳細が明らかにされている。即ち、プロリン水酸化酵素が、ＨＩＦ－１αタンパク質の中央付近にあるＯＤＤドメインのプロリン残基を水酸化し、これを目印にして結合するユビキチン連結酵素複合体Ｅ３により、ＨＩＦ－１αはユビキチン化されプロテオゾームに運ばれて分解される。このプロリン水酸化酵素が機能する際に、酸素を含んだ鉄分子を必要とすることが酸素依存性の中枢機構であった。このＯＤＤ制御は極めて厳密で、低酸素下で安定化したＨＩＦ－１αは、有酸素にすると数分以内に分解される。この極めて厳密なＯＤＤ制御機構を応用して、低酸素がん細胞特異的イメージング・ターゲティング材料の構築が始まった。

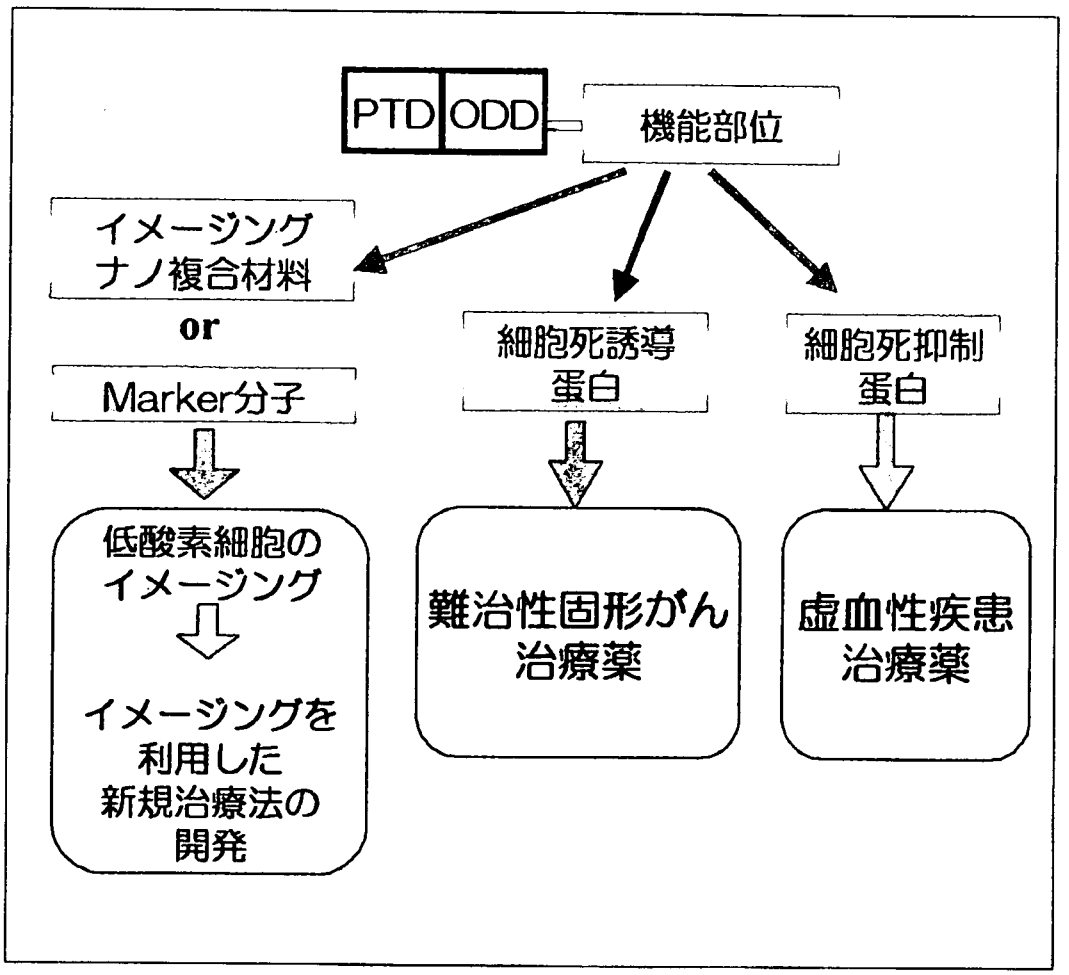

図3　PTD-ODD融合タンパク質の利用例

3. ＰＴＤ－ＯＤＤ融合タンパク質の構築

我々がまず行ったことは、上記のＨＩＦ－１αにあるＯＤＤドメインを任意のタンパク質に融合させることで、任意のタンパク質が持つ機能を酸素濃度依存的に制御することができるか否かの検証である。ＯＤＤドメイン全部（約２００アミノ酸）を付加すると、全体の分子量がかなり大きくなるので、最小のアミノ酸配列を決定するためにＯＤＤドメインを部分的にβ－ガラクトシダーゼに融合させ、β－ガラクトシダーゼ活性の酸素濃度依存性を調べた（図２）。その結果、少なくとも18個のアミノ酸があれば、任意のタンパク質の活性をＯＤＤ制御できること、最適なＯＤＤ制御のためには、約50個のアミノ酸配列からなるＯＤＤドメインが必要であることがわかった。

ＯＤＤ制御できるタンパク質が作れても、細胞内に導入できなければ、細胞内で行われ

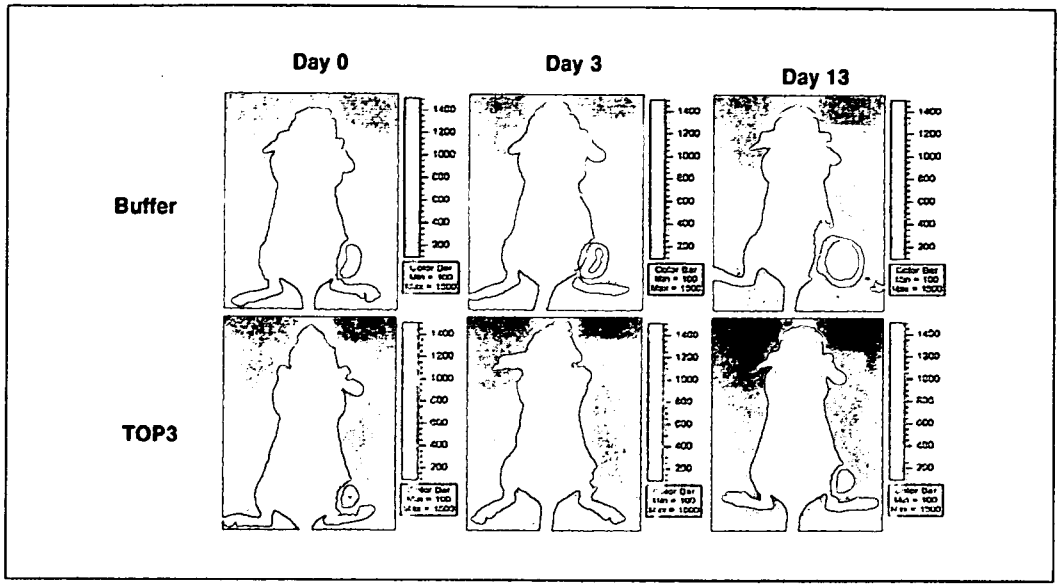

図4　TOP3による抗がん効果
光イメージングにより低酸素領域を可視化する系で同一マウス大腿部腫瘍内の低酸素がん細胞の量を経時的にモニターした。TOP3の投与は20mg/Kg，day0，5，10の3回。

るＯＤＤ制御を受けることができない。そこで我々は、タンパク質に膜透過性を付加する膜透過ドメイン（ＰＴＤ）をＯＤＤ融合タンパク質に付加することにより、培養細胞を用いた実験でほぼ100％の細胞にタンパク質を導入し、酸素依存的に機能させることに成功した。しかもこのＰＴＤ融合タンパク質は、ネズミの腹腔内に投与すると、脳を含む全身の組織細胞にデリバリーされることが示されている。そこで我々は、ＰＴＤ－ＯＤＤ－β－ガラクトシダーゼを腹腔内に投与し、この融合タンパク質の体内分布とβ－ガラクトシダーゼ活性を調べた。その結果、ＯＤＤを付加していないタンパク質を投与した場合、正常肝組織と腫瘍組織全体で、タンパク質と活性が確認できたのに対し、ＯＤＤを付加したタンパク質を投与した場合は、正常組織ではタンパク質も活性も確認できず、腫瘍組織でも一部でのみタンパク質と活性が確認できた。その部分が低酸素であるか否かを確認するために、低酸素マーカーとして知られている化合物（pimonidazole）を用いて腫瘍切片を染色したところ、低酸素マーカーと同一のところに、β－ガラクトシダーゼタンパク質が存在していることがわかった。これらの結果は、我々の設計通り、ＰＴＤ－ＯＤＤ融合タンパク質はＯＤＤ制御を受け、低酸素がん細胞特異的に分布・機能することを示しており、低酸素がん細胞特異的イメージング・ターゲティングが可能であることを示していた。

4．ターゲティングへの応用

ＰＴＤ－ＯＤＤ融合タンパク質は、機能ドメインに付加するものを変えることで、様々な機能を持たせることができる（図3）。即

ち、低酸素がん細胞に細胞死を誘導する機能を付加することで、低酸素がん細胞のターゲティングを行うことができる。モデルタンパク質として構築したＴＯＰ３は、低酸素細胞内で安定化し、活性化され細胞死を誘導するように設計されている。ＴＯＰ３を投与することにより、腫瘍サイズは小さくなった。ヒト膵臓がん細胞をネズミの皮下に移植した実験で、無処理群で腫瘍体積が２倍になる日数が4.8 ± 2.3日であったのに対し、ＴＯＰ３投与群では、12.6 ± 5.4日（＊ｐ＜０．０３）と約３倍にのびている。この明らかな腫瘍増殖抑制効果の原因が低酸素がん細胞を効率よく腫瘍から除いているためであることが、腫瘍内低酸素がん細胞を光イメージングで可視化し、経時的に観察することにより明らかになった（図４）。今後臨床応用にむけて検討を行っていく予定である。

5. イメージングへの応用

タンパク質を用いる場合は光イメージングが最も容易で種類も多いが、光の透過度が小さいことから光イメージングの臨床応用は現状では極めて難しい。しかしながら、基礎的データが容易に集められることから、現在機能ドメインに光イメージングに対応する物を融合させて動物実験を行っている。将来的には、磁性体ナノ粒子の利用を検討しており、ＭＲＩによる低酸素がん細胞の画像化をめざして研究を進めている。

おわりに

「西暦2015年には、１年間に89万人ががんにかかる（がんセンターＨＰ）」と予測されている。1990年代で既に、男性では55%、女性では65％が5年以上生存している。つまり、毎年がん治療を受けて治った約50万人が、その後再発と転移の不安をかかえながら、長い人生を歩む時代が来たといえる。定期的なモニターによるがんの早期発見は、このようなハイリスク群のみならず、通常の検診でがんの早期発見を望んでいる予備群に対しても重要であることは言うまでもない。

現在の画像診断では、基本的に正常組織との違い（異常）を探し出すことで、がんを検出する手法が取られるため、小さな癌を見つけるためには、かなりの知識と経験が求められる。それでは、とても急増する需要に追いつくことができない。そのためにも誰が見ても明らかにがんの存在を示唆できるような鮮明な画像を提供できるプローブの開発が必須である。つまり、「がんが無ければ画面には何も写らず、イメージとして画面に写し出されたら、そこにがんがある」という極めて簡単な画像診断を提供でき、しかもがんの組織特異性に左右されず、どのようながんでも早期に検出が可能であるプローブ、そんな夢のようなプローブを我々は、これまでに医学の領域では使われることのなかった工学系の材料；ナノ複合材料を応用することで実現しようとしている。革新的診断・治療への挑戦である。

参考文献

1) Kizaka-Kondoh S, Inoue M, Harada H and Hiraoka M. Tumor hypoxia: a target for selective cancer therapy. Cancer Science. 94, 1021-8 (2003).Review.
2) Harris AL. Hypoxia - A key regulator factor in tumor growth. Nature Rev. Cancer;2:38-47.(2002). Review.
3) Schwarze SR, Ho A, Vocero-Akbani A, Dowdy SF. In vivo protein transduction: delivery of a biologically active protein into the mouse. Science. 285,1569-72. (1999).
4) Semenza GL.HIF-1, O(2), and the 3 PHDs: how animal cells signal hypoxia to the nucleus. Cell. 107,1-3. (2001). Review.

4．癌治療における HIF-1 と Tumor Hypoxia

近藤　科江*　平岡　真寛**1)　原田　浩**

Hypoxia-inducible factor 1（HIF-1）は，低酸素応答転写因子として見いだされ，固形腫瘍における血管新生，糖代謝，転移・浸潤等に関与する多くの遺伝子の発現を誘導し，がんの悪性化やがんによる死亡率上昇に深く関わっている事がわかってきた。基礎研究レベルでは，HIF-1 を抑制することで，がんの増殖が抑えられるという報告が多数あり，HIF-1 の活性を抑制するための研究が，抗がん治療において注目され始めている。ここでは，最近の HIF-1 研究と，HIF-1 を標的にしたがん治療戦略を我々の研究を含めて紹介したい。

Ⅰ．Tumor Hypoxia と HIF-1

がんを構成するがん細胞の性質を知ることは，がんを治療する上で極めて重要である。分子生物学の発展とともに，がん研究は，細胞レベルから分子レベルに移行し，分子標的が抗がん治療において大きな注目を集めている。一方で，腫瘍全体の構造的特徴からくる腫瘍内環境いわゆる微小環境（microenvironment）が，がん細胞の性質を大きく変えているということが分子レベルでも明らかになり，がんを治療するうえで考慮すべき極めて重要な研究テーマとして，注目され始めている。

がんの微細環境は，低酸素，低 pH，低ブドウ糖濃度等により特徴づけられている。がん細胞の無秩序な増殖が極めて不規則な血管新生を引き起こし，不完全な血管構造と分布によって引き起こされる慢性（chronic）および急性（acute）の虚血領域が生じる[1]。慢性的な虚血状態は，がんの増殖に血管新生が追いつかない結果引き起こされる。血管から供給される酸素や栄養が細胞を維持できるのは，たかだか 100 μm 前後と言われており，それ以上血管からの距離が離れた位置にあるがん細胞は，虚血状態にあり，更に距離がはなれると細胞は壊死してしまう（図１）。この壊死細胞に隣接する瀕死の虚血がん細胞が，実はがんの悪性に深く関わっている事が，最近の研究からわかってきた[2～4]。

“瀕死の虚血がん細胞”が分布している領域は，低酸素状態にあるために腫瘍内低酸素領域（Tumor

* *Shinae Kizaka-Kondoh*　京都大学大学院医学研究科放射線腫瘍学・画像応用治療学 COE 助教授
** *Masahiro Hiraoka, Hiroshi Harada*　京都大学大学院医学研究科放射線腫瘍学・画像応用治療学　教授

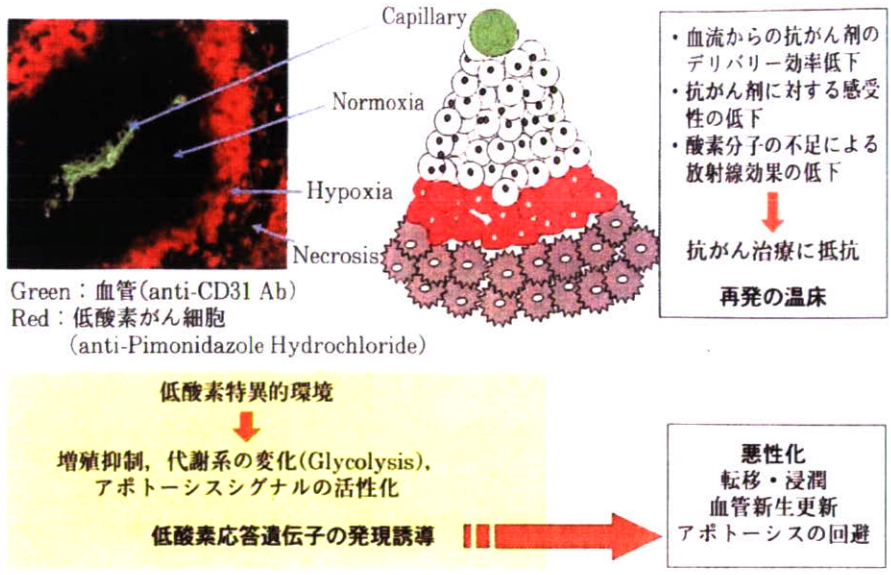

図1　がんの微小環境

腫瘍切片を血管（緑）と低酸素がん細胞（赤）を認識する抗体で免疫染色すると，低酸素領域は，血管から100μm程度離れた領域に，壊死領域を取り囲むように帯状に存在することがわかる（左上図）。低酸素がん細胞は，抗がん剤が届きにくい上に増殖が抑えられているため薬剤耐性であり，放射線にも抵抗性である。また，低酸素がん細胞で活性化するHIF-1により誘導される遺伝子の機能により，腫瘍全体の増殖・悪性化を亢進する（本文参照）。

hypoxia），“瀕死の虚血がん細胞”は低酸素がん細胞（hypoxic tumor cells）と呼ばれている。低酸素がん細胞は，「瀕死状態」ではあるが，その劣悪な環境に適応しようと努力している。その努力の一翼を担っているのが低酸素応答転写因子として単離されたhypoxia-inducible factor 1（**HIF-1**）である。HIF-1は，低酸素条件下で速やかに活性化され，糖代謝や糖輸送に関与する遺伝子の発現を誘導したり，血管新生因子や増殖因子の発現を促進したりして，栄養環境の改善を図る。アポトーシスの回避や，遺伝子変異を誘導する遺伝子の発現をうながして，死を免れようとする。その一方で，転移や浸潤に関わる遺伝子の発現を誘導して，自ら新天地を切り開こうとする。このような一連の「生き残り」のための行動が，がん全体の悪性化に繋がっていたのである[5~7]。また，低酸素領域の構造的な要因で，低酸素がん細胞は，がん治療に対して抵抗性である[7]。血流にのって運ばれる抗がん剤は，血管から遠い低酸素がん細胞までは効率よく運ばれないため，治療に有効な濃度に達する機会が少ない。また，多くの抗がん剤は，分裂している細胞を標的にしているため，増殖を停止している低酸素がん細胞では有効に作用しない。更に，酸素分子により細胞死誘導能が増強される放射線やある種の抗がん剤は，低酸素条件下ではその治療効果が十分に発揮できない。したがって，放射線や抗がん剤治療の後に，周辺の活発に分裂していたがん細胞が死滅しても，低酸素がん細胞は生き残る場合があり，治療不良・再発の原因となることが示唆されている[5,7]。一方で，固形腫瘍内の低酸素領域の酸素濃度は，無酸素状態（0％）に隣接するところまで続いており，正常組織にあり得ない低酸素状態にあるがん細胞が存在するため，腫瘍特異的標的になりうる。

Ⅱ．HIF-1の制御機構

1992年にSemenzaとWangによって低酸素応答転写因子HIF-1の存在が報告され[8]，1995年に単離・精製されて[9]以来，分子レベルの研究が加速度的に進み，HIF-1の機能とがんとの関わりが次々に明らかになってきた。HIF-1によって直接発現が誘導される遺伝子

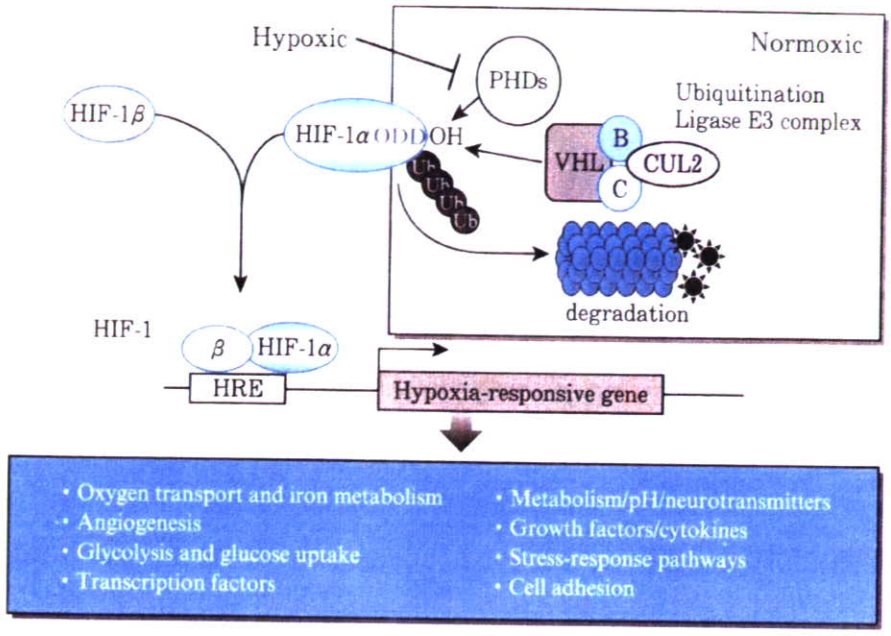

図2　HIF-1αの酸素依存的分解制御

有酸素細胞内では，プロリン水酸化酵素（PHDs）によって修飾され，ユビキチン化酵素（Ubiquitin-ligase E3 complex）がその修飾を認識して，VHL を介して結合する。ユビキチン化された HIF-1α はプロテアソームで分解される（右上図）。PHDs は酸素を必要とするため，低酸素細胞内では機能せず，HIF-1α は安定化する。低酸素細胞内では，HIF-1α は HIF-1β と結合して，転写因子 HIF-1 を形成し，様々な遺伝子の発現を誘導する。

の同定が盛んに行われ，現在までに既に 60 以上が報告されている[5]。これらの遺伝子は，プロモーター，エンハンサー領域に HIF-1 結合配列 hypoxia-responsive element（**HRE**）を持っており，HIF-1 が p300/CBP とユニットを作って HRE に結合し転写を促す。

HIF-1 は，αβの異なる 2 つのサブユニットからなる（**図2**）。βサブユニット（**HIF-1β**）は恒常的に発現しているが，αサブユニット（**HIF-1α**）の発現量は翻訳後修飾と翻訳レベルで厳密に制御されている（**図3**）。従って HIF-1 の活性は HIF-1β に結合できる HIF-1α がどのくらい存在するかに依存している。HIF-1α の翻訳後修飾による制御は，酸素依存的なプロリン水酸化酵素（**PDHs**）により主になされているが，腫瘍によっては，p53-Mdm2 による制御も報告されている[10]。転写活性制御は酸素依存的なアスパラギン酸水酸化酵素（**FIH**）による抑制と，mitogen-activated protein kinase（**MAPK**）を介する活性化が知られている。翻訳レベルの制御は酸素非依存的で，増殖因子等による phosphatidylinositol 3-kinase（**PI3K**）や **ERK**（extracellular-signal-regulated kinase）を介するシグナル伝達系の活性化が関与している。

1．プロリン水酸化酵素を介する HIF-1α タンパク質制御

HIF-1α が有酸素状態の細胞内で分解される機構は，2001 年に PHDs がクローニングされることによって，ほぼ全容が解明された[11]。有酸素状態の細胞内では，HIF-1α の 402 と 564 番目のプロリン残基が PHDs により翻訳後修飾を受け目印が付けられる。この目印をめがけて E3 ubiquitin-ligase complex が von Hippel-Lindau（**VHL**）を介して結合する事で Ubiquitin-mediated degradation が起こり，HIF-1α はプロテアゾームで分解される（**図2**）。即ち，有酸素状態の細胞（通常の酸素状態にある細胞）では，HIF-1α タンパク質は常に作られ，即時に壊されるという不経済なタンパク質ではあるが，細胞が低酸素等のス

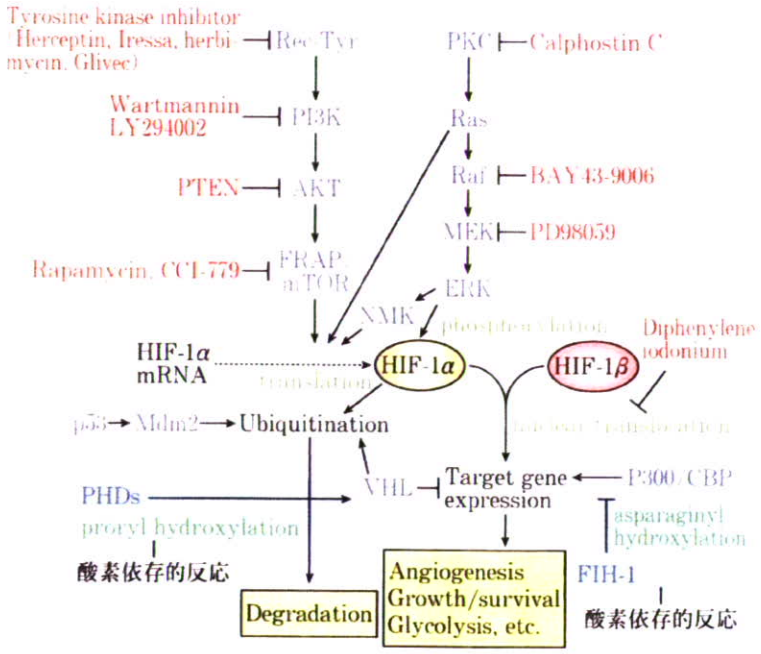

図3　HIF-1の発現・活性の制御機構と阻害物質
HIF-1の制御に関わる因子を青字で，それらの阻害物質を赤字で示してある。
詳細は本文参照。

表1　HIF-1活性の制御機構

タンパク質分解	プロリン水酸化酵素	↑ユビキチン化	酸素依存的 / 細胞非特異的
	P53-Mdm2	↑ユビキチン化	酸素非依存的 / 細胞特異的
転写活性抑制	アスパラギン酸水酸化酵素	↓C末転写活性	酸素依存的 / 細胞非特異的
転写活性上昇	Raf-MEK-ERKシグナル	↑HIF-1/p300複合体形成	酸素非依存的 / 細胞特異的
翻訳レベル上昇	PI3K-Akt-mTORシグナル	↑eIF-4E活性	酸素非依存的 / 細胞特異的
翻訳レベル上昇	Raf-MEK-ERKシグナル	↑eIF-4E活性	酸素非依存的 / 細胞特異的

トレス状態になった場合に，即座に対応できるように準備されているSOS的な存在であると考えられる。PHDsはヒトでは3遺伝子がクローニングされており[11]，有酸素状態の細胞で主にHIF-1αの分解を担当しているのはPHD2であるという報告がある[12]。PHDsの機能は酸素濃度依存的である(**表2**)が，必ずしも絶対酸素濃度により決定されている訳ではない。ヒトの組織の酸素濃度は，各々至適酸素濃度があり，例えば通常の酸素濃度が20%に近い組織では，5%にまで酸素濃度が下がるとHIF-1αの発現が確認できるようになる一方で，通常の酸素濃度が5%程度の組織では，その濃度でもHIF-1αの発現が認められない。つまり，PHDsの機能は，各々の組織細胞において，「異常に低い酸素濃度だ」とPHDsが察知した時に機能していると考えられる。

2．アスパラギン酸水酸化酵素を介する転写活性制御

HIF-1αの転写活性ドメインTAD-Cに存在する803番のアスパラギン酸を水酸化する酵素FIH-1(factor inhibiting HIF-1)は，有酸素状態の細胞内でHIF-1αを水酸化する事によりp300/CBPとHIF-1αとの結合を阻止し，転写活性を抑制する[13]（**表1**）。FIH-1は更にVHLとも結合し，histone deacetylaseをHIF-1αにリクルートすることにより，有酸素状態でHIF-1の転写活性を抑制することが報告されている[13]。

表2　HIF-1 活性を制御する水酸化酵素

	細胞内分布	mRNA 誘導	HIF-1α核内移行	機能 / 備考
PHD1	核	酸素非依存的	阻害する	低酸素での HIF-1α の分解 /estrogen により誘導
PHD2	細胞質	↑酸素依存的	阻害する	低酸素下で Siah2 により分解 有酸素での HIF-1α の分解 / 低酸素で発現上昇
PHD3	細胞質と核	↑酸素依存的	阻害する	低酸素での HIF-1α の分解 / 低酸素下で Siah2 により分解
FIH1	細胞質	酸素非依存的	阻害しない	有酸素での転写活性阻害 / 発現量は酸素非依存的

3．翻訳レベル制御

EGFR や PDGFR 等のチロシンキナーゼ受容体および下流のシグナル伝達因子は，がん遺伝子として同定されている物が多く，ヒト腫瘍におけるこれらの因子の変異や過剰発現は珍しくない。そのような腫瘍で，HIF-1α の発現量が増え，HIF-1 活性が上昇したという報告が多数ある。たとえば，PTEN の loss of function mutant による PI3K-AKT-mTOR を介するシグナルの亢進や，*Ras* や *Raf* 癌遺伝子の変異による Raf-MEK-ERK シグナル亢進が HIF-1 の翻訳レベルを上昇させる（図3）。HIF-1α の翻訳レベル制御が，上述した翻訳後修飾と異なる点は，酸素非依存的である事に加えて，細胞特異性がある事である（表2）。この細胞特異性は，HIF-1α の発現量を上昇させる PI3K-AKT-mTOR や RAF-MEK-MAPK のシグナル伝達系（図3）を活性化する条件，つまり増殖因子やサイトカイン，その他の活性化因子の量やがん遺伝子の活性化の状態に依存していると考えられる。HIF-1α の発現量が増えることによって，上記の酸素依存的分解を上回る量の HIF-1α タンパク質が細胞内に存在すると，有酸素状態の細胞でも HIF-1 転写活性が見られるようになり，がんの悪性化に関与する遺伝子の発現が誘導される。

Ⅲ．HIF-1 活性の可視化

以上のように，固形腫瘍内の HIF-1 活性は，がん治療，特に難治性のがんにおいて，極めて重要な因子であり，抗がん治療効果を高め，再発・悪性化を予防するためには，固形腫瘍内の HIF-1 活性の分布を明確にするモニター手法が望まれている。現在，腫瘍内 HIF-1 活性をモニターするために，前述した HIF-1 結合 DNA 配列 HRE を含んだレポーターベクターを用いる方法がとられている。レポーター遺伝子としては，蛍光タンパク質や化学発光をおこすルシフェラーゼタンパク質をコードしている遺伝子が用いられている[14, 15]。我々は，5個の HRE を持つプロモーターの下流にルシフェラーゼ遺伝子を繋いだレポーターを組み込んだヒトがん細胞を用いて HIF-1 活性をモニターする系を構築した[16]（図4A）。レポーターを組み込んだヒトがん細胞をヌードマウスに移植すると，形成した腫瘍内の低酸素環境に応答してルシフェラーゼタンパク質が発現され（図4B）基質であるルシフェリンを投与後一定期間，発光反応を起こす。この化学発光を，冷却高感度 CCD カメラを搭載したイメージング機器 in vivo imaging system（IVIS）を用いて可視化することができる（図4C）。つまり，このシステムを用いることにより，同一担がんマウスの固形腫瘍内低酸素領域の変化を定量的に，リアルタイムで，何度でも経時的に観察することが可能である[16]。しかも発光シグナルを定量することにより，低酸素がん細胞の増減を数量化したデータとして推移を観察することができる。この系が確かに腫瘍内の低酸素状態をモニターしていることを確認する目的で，腫瘍を形成した下肢を縛ることで血行を悪くして，物理的に低酸素領域を増やす操作を行った（図4C）。腫瘍内のルシフェラーゼ発現を IVIS で経時的に観察したところ，HIF-1 活性が時間とともに上昇し，低酸素領域が増加していることが確認できた[16]。

Ⅳ．がん治療の標的としての HIF-1

HIF-1α の過剰発現が，HIF-1 転写活性の増強に繋がり，がんの悪性化に関与する遺伝子の発現を誘導することにより，がんによる死亡率を上げることにな